Title:
Observability measures for the longitudinal dynamics of railway vehicle bogies

Authors:
Christoph Schwarz, Andreas Heckmann, Benjamin Heckmann

Book:
Dynamics of Vehicles on Roads and Tracks: Proceedings of the 25th International Symposium on Dynamics of Vehicles on Roads and Tracks (IAVSD 2017), 14-18 August 2017, Rockhampton, Queensland, Australia

Editors:
Maksym Spiryagin, Timothy Gordon, Colin Cole, Tim McSweeney

Observability measures for the longitudinal dynamics of railway vehicle bogies

C. Schwarz & A. Heckmann
German Aerospace Center, Oberpfaffenhofen, Germany

B. Heckmann
Knorr-Bremse Systeme für Schienenfahrzeuge GmbH, Munich, Germany

ABSTRACT: In the current work a new, signal based observability measure is proposed and applied. This measure surveys the observability from the signal analysis point of view. In contrast to existing measures it can be computed for nonlinear systems and makes no stringent requirements on the signal properties. As an example for a highly nonlinear system a railway bogie model is implemented that comprises a nonlinear wheel-rail contact formulation. The newly developed index is evaluated with regard to the longitudinal dynamics of the bogie and in this way the index allows for a reasonable choice of the most meaningful sensor signals. Finally, a comparison with already existing indices illustrates the benefits and weaknesses of the new observability measure.

1 INTRODUCTION

Safety and comfort or at least one of them are major topics of most research activities that deal with passenger transport, whether on roads or on tracks. Regarding the longitudinal dynamics of railway vehicles the wheel-rail contact is the crucial point for safety as well as comfort. Hence, a controller for the longitudinal dynamics would help to minimize the impact of the time- and path-dependent friction conditions, which complicate a smooth longitudinal motion over the entire train set. However, to enable an advanced feedback controller, the actual dynamics acting in the bogie system have to be determined or rather estimated, since a direct measurement of all relevant dynamics is usually not feasible due to technical and economic reasons. Finally, to obtain reliable and accurately estimated information, the observer setup requires a suitable choice of both the measured signal and the sensor position.

There are some control theoretic observability indices, e.g. the index introduced in Lückel & Müller (1975), which quantify the observability of a certain sensor configuration. In contrast to this modal index, which relies on the observability of the system eigenvalues, the methods described in Benninger & Rivoir (1986), Hac & Liu (1993) and Lystianingrum et al. (2014) give information on the observability of the physically meaningful dynamic states of the system. A major drawback of these indices is their limitation to linear systems. In case of a highly nonlinear system like a railway bogie with the complex wheel-rail contact dynamics the abovementioned indices might lead to inaccurate results.

In the current work, an index is established that rates the observability in terms of signal analysis and accordingly rests on the simulation data of a detailed nonlinear system. Therefore, chapter 2 presents a nonlinear and a linearized model of a bogie. Chapter 3 describes the calculation of the newly developed observability measure and illustrates its application to the longitudinal dynamics of the railway bogie. Furthermore, a comparison is drawn between the results of the new measure and two state-of-the-art measures. At the end, a conclusion is drawn and an outlook on the upcoming tasks is given.

2 DESIGN OF BOGIE MODELS

2.1 *Nonlinear 3-D bogie model*

In this subsection a detailed 3-D model of a railway bogie is described, that will be used later on for the calculation of the new observability measure. The multibody simulation tool Simpack is utilized to generate the bogie model. The configuration of the bogie is based on extensive enquiries about modern and commonly used bogie types, see Siemens (2017), Bombardier (2007, 2008a, b) and Alstom (2015). Thus, a trailer bogie is chosen that is equipped with two axle brake units per wheelset, wing guidances for the wheelsets and a lemniscate guidance between bogie and car-body, see Figure 1a. The multibody model comprises 36 bodies with at least 51 degrees of freedom. All parts of the bogie are assumed to be rigid bodies and the FASTSIM algorithm, see Kalker (1982), is chosen to calculate the wheel-rail contact dynamics. The suspension parameters are based on the results described in Iwnicki (1998) and adapted for a high speed bogie configuration. In the end, the detailed 3-D model is not only used for the evaluation of the new observability index but also to validate the 2-D model described in the following subsection. Furthermore, it might be used to optimize the observer, what is, however, not part of the presented work.

2.2 *Linear 2-D bogie model*

The linear bogie model is implemented using the equation based modeling language Modelica. Modelica offers some benefits like multi-physical system design and advanced features in the control and observer synthesis. With the help of the *Modelica_LinearSystems2* library, the linear model is directly output in state-space representation by linearizing and transforming a nonlinear multibody model. The advantage of this approach is that the initially designed multibody model can readily be used as observer system and an Extended Kalman Filter might be generated, see Brembeck et al. (2014). Thus, the multibody model is structurally based on the bogie configuration described in the previous section. However, the system is implemented as a planar 2-D model, see Figure 1b, that neglects the lateral, yaw and roll motions, since the focus of this work is on the longitudinal dynamics. Furthermore, the Polach contact formulation is utilized, see Polach (1999). In the end, further simplifications of the brake components and the force elements lead to a system with eleven degrees of freedom and seven rigid bodies, that is approximately a fifth of the size of the nonlinear model illustrated above.

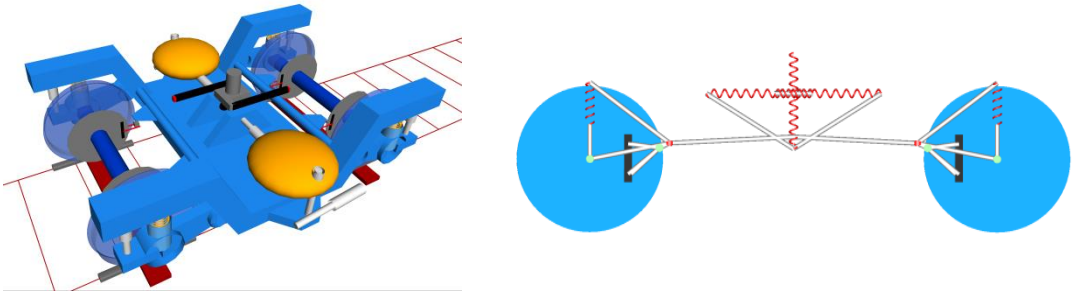

Figure 1. a) Detailed 3-D multibody model in Simpack; b) Planar 2-D multibody model in Modelica.

3 APPLICATION OF OBSERVABILITY MEASURES

3.1 *Derivation and application of the envelope index*

In the following, the calculation of the new observability index is described in detail and it is applied to the longitudinal dynamics of the nonlinear bogie system presented in section 3.1. The index is based on the cross-correlation of two signals, see Bendat & Piersol (1993). These signals are on the one hand a signal x that cannot be measured in a real application and on the other hand a signal y that might be an input of an observer. The index calculation is done as follows:

1. Shift y in the time domain to y_{lag} with the lag identified via $\tau_{lag} = \max_\tau((x \star y)(\tau))$.

2. Define the envelopes h_h and h_l, that uniquely allocate the highest and lowest values of y_{lag} to each x and vice versa.
3. Search for the maximum distances Δx_{max} and Δy_{max} between h_h and h_l

$$\Delta x_{\max} = \max_{y_{lag}} \left| h_h(y_{lag}) - h_l(y_{lag}) \right|, \Delta y_{\max} = \max_{x} \left| h_h(x) - h_l(x) \right|. \quad (1)$$

4. Calculate the envelope index e_O as

$$e_O = 1 - \frac{1}{2}\left(\left| \frac{\Delta x_{\max}}{x_{\max} - x_{\min}} \right| + \left| \frac{\Delta y_{\max}}{y_{\max} - y_{\min}} \right| \right). \quad (2)$$

According to other normalized measures the envelope index tends to a value of one in case of a good observability and to zero when y shows no distinct relation to x.

As mentioned above e_O is now evaluated to rate the observability of the longitudinal dynamics of a railway bogie. Thus, the longitudinal force F_{RW} in the wheel-rail contact is defined as signal x and five different signals are tested as potential observer inputs y, see Table 1. To identify potential dynamic interdependencies between two bogies linked by a car-body, not a sole bogie is simulated but an entire wagon with two identical bogies.

Table 1. List of tested observer inputs y.

Bogie pitch angle	β_B
Deflection of the secondary spring	Δz_S
Strain of the lemniscate guidance	Δx_L
Longitudinal acceleration at the car body	a_{Cx}
Longitudinal acceleration at the bogie	a_{Bx}

The first scenario to be evaluated is a braking process lasting 33 s with a linear fade-in and fade-out and a short-time anti-slide overlay. Furthermore, the bogie system is excited by track irregularities according to ERRI low, see ERRI (1993). Figure 2 illustrates the time domain results of F_{RW} by the solid line as well as the five already time shifted sensor signals $y_{i,lag}$. The rail-wheel force can be divided into three characteristic phases: a regular phase $t = [12\,s, 29\,s] \cup [33\,s, 40\,s]$, the overbraking period $t = [29\,s, 31\,s]$, where the wheel rotation overcritically decreases and finally the anti-slide phase for $t = [31\,s, 33\,s]$, where F_{RW} falls to nearly zero. The various $y_{i,lag}$ provide different levels of congruence to F_{RW} in the specific phases. To illustrate this and to highlight the graphical meaning of the envelope index, Figure 3a shows β_B and Δx_L plotted against F_{RW}. Regarding the dashed line β_B, Δy_{max} occurs at $F_{RW} = 0$, i.e. during the anti-slide phase. Δx_{max} is also associated to the anti-slide overlay, since β_B drops only to approximately 50% of its maximum value. The dotted line describing Δx_L pictures a completely different trend, as Δy_{max} is caused by the overshoot right after the anti-slide phase, see Figure 2. Furthermore, Δx_{max} might mainly be founded in the rail irregularities, since the drops in F_{RW} during the overbraking phase and the anti-slide overlay are well imitated.

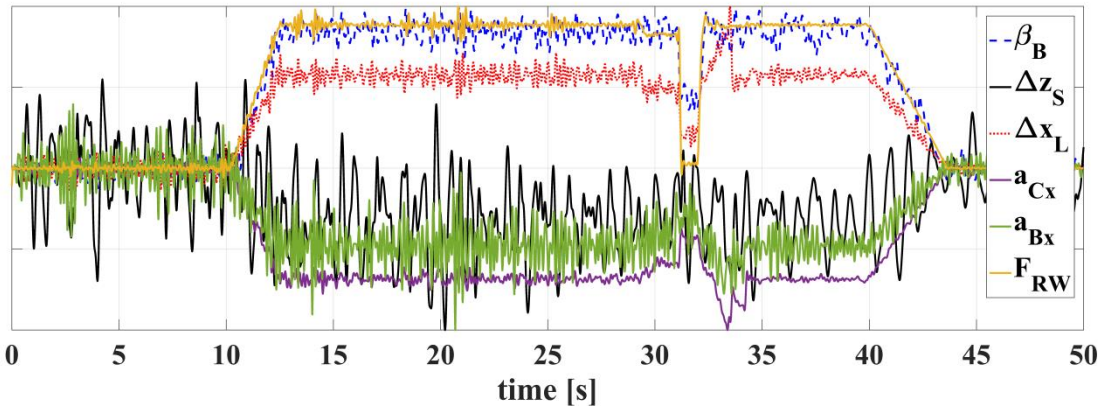

Figure 2. Time domain results of realistic brake scenario.

In a second scenario, a sine sweep with constant amplitude and a frequency range [0.1 Hz, 5 Hz] is applied as brake excitation and the track is assumed to be ideal, i.e. no irregularities are considered. This approach allows for a frequency dependent assessment of the observability. Figure 3b depicts the results of Δz_S against F_{RW}, with the color coded with respect to the frequency. Thus, at low frequencies, illustrated in blue, the correlation is almost ideally linear apart from a slight hysteresis. However, at high frequencies Δz_S remains on a constant level disregarding the changes in F_{RW}. This behavior arises from the pitch inertia of the car body and disqualifies Δz_S as observer input at least for the detection of high-frequency longitudinal dynamics. After the illustration of two different perspectives and use cases, respectively, the envelope index is in the following subsection compared to other observability measures and its benefits as well as its weaknesses are discussed.

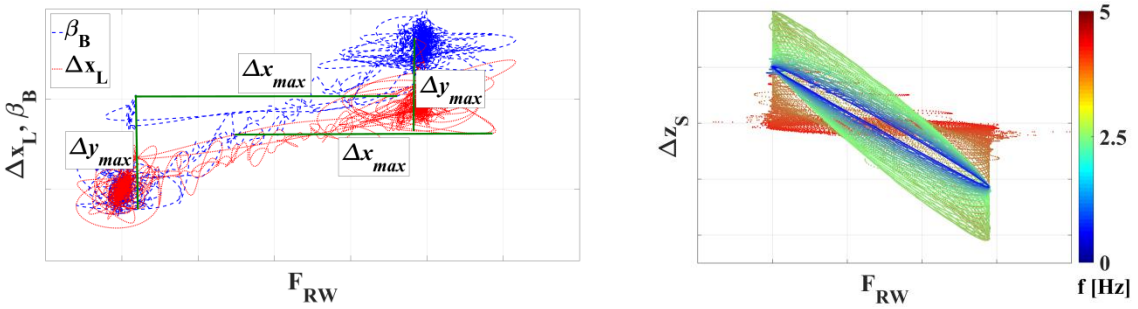

Figure 3. Exemplary graphical interpretation of e_O in case of realistic brake scenario (a: left) and sine sweep excitation (b: right).

3.2 *Comparison between envelope index and linear observability measures*

The envelope index is opposed to two measures, each referring to one of the two bogie systems described in chapter 2. On the one hand a state-of-the-art observability measure based on a linear system is used, as stated by Benninger & Rivoir (1986). On the other hand the signal based cross-correlation coefficient is consulted using the same simulation data as for the calculation of e_O, see for example Bendat & Piersol (1993). Firstly, the linear index m_{Ok} is described and evaluated that weights the observability of the system state z_k for a specific sensor configuration, with $k \in \{1, N\}$ and N the number of states. The calculation of m_{Ok} refers to the observability Gramian $\underline{Q}_O$

$$m_{Ok} = \left\{ \left(\underline{Q}_O^{-1} \right)_{kk} \right\}^{-\frac{1}{2}}, \text{ with } \quad \underline{Q}_O = \int_{t_0}^{t_1} e^{\underline{A}^T (t_0 - \tau)} \underline{C}^T \underline{C} e^{\underline{A}(t_0 - \tau)} d\tau , \tag{3}$$

the system matrix $\underline{A} \in \mathbb{R}^{N \times N}$ and the output matrix $\underline{C} \in \mathbb{R}^{p \times N}$. The evaluation of the bogie dynamics is illustrated in Figure 4a. The ten columns represent the normalized sums over the bogie states related to the longitudinal dynamics, since the wheel-rail force is not defined as a state and therefore m_{Ok} cannot be calculated with respect to F_{RW}. In addition to the denoted signals the angular wheel velocity ω_W is part of each and every presented sensor configuration, i.e. $\underline{C}$ contains ω_W as well as one of the five named alternatives. If only the five denoted signals would be detected, the linear system becomes unobservable in control theoretic terms and the results could not be meaningfully compared to the envelope index.

The results marked black in Figure 4a belong to a system linearized at a low longitudinal velocity and the results marked grey to a system with a high longitudinal velocity. Firstly, the different observability levels of the systems for β_B, Δz_S and Δx_L are conspicuous and, secondly, the variable slopes for the accelerations a_{Cx} and a_{Bx}. As these differences between the structurally identical systems indicate, this measure might not work very well for systems with major nonlinearities. Furthermore, the calculation of m_{Ok} requires stable dynamics and the inversion of $\underline{Q}_O$ might not work properly in case of badly conditioned system matrices. Another drawback of this index might be that it rates the dynamic effect dependent on the sensor type. For example the deflection of springs would be evaluated differently whether it is detected via a force or a

displacement sensor due to the divergent values in the output matrix $\underline{C}$. The envelope index avoids this problem by dividing Δx_{max} and Δy_{max} by (x_{max} - x_{min}) and (y_{max} - y_{min}), respectively. In the end, the requirements on the system as well as on $\underline{Q}_O$ are severe restrictions that might not be met by more and more complex systems. Nevertheless, this index allows benchmarking an entire sensor concept at once, whereas the envelope index in its current version rates only specific signals.

The second method to rate the observability is the cross-correlation coefficient c_{xy}, which gives information on the linear dependency between the two signals x and y. The calculation of c_{xy} depends on the mean values $\bar{y}$ and $\bar{x}$

$$c_{xy} = \frac{\sum_{i=1}^{L}\left((x_i - \bar{x}) \cdot (y_i - \bar{y})\right)}{\sqrt{\sum_{j=1}^{L}(x_j - \bar{x})^2 \cdot \sum_{l=1}^{L}(y_l - \bar{y})^2}}, \tag{4}$$

with L as the length of the sampled signals. The normalized results of c_{xy} are depicted together with e_O in Figure 4b, both evaluating the first braking scenario described in the previous subsection. As it is stated in Bendat & Piersol (1993), the correct calculation of the cross-correlation coefficient demands ergodic signals, i.e. the signals have to be stochastic and their mean values might not vary over time. Since this requirement is not met in the current scenario, c_{xy} provides some essential derivations with respect to e_O. First of all, c_{xy} rates β_B, Δx_L and a_{Cx} on the same level, whereas e_O shows an optimum for Δx_L. As described in the discussion of Figure 3a there are some characteristic differences between β_B and Δx_L, so benchmarking them on the same level would disregard this information. Another deviation can be seen for a_{Bx}, that is rated almost as good as Δx_L in case of c_{xy} but almost as low as Δz_S in case of e_O. This fact comes from the higher weighting of single outstanding events in e_O like the anti-slide overlay in the current scenario. A feature that both approaches share is the consideration of process noise that allows for a meaningful benchmark of potential observer inputs in terms of signal analysis.

Considering the results of e_O in Figure 4b the measurement of the lemniscate strain Δx_L and, if possible, also the bogie pitch angle β_B might be used to achieve the best observability of the longitudinal dynamics of a railway bogie. To assure the observability rating of e_O it is recommended to simulate different scenarios and average their results, that would however have exceeded the scope of the present work. To sum up, the major advantage of the new index is its generality, since it does make requirements neither on the system nor on the signals that are compared. However, the envelope index is not consistent to the control theoretic meaning of observability, so a control theoretic observability check of the favored sensor configuration is advised.

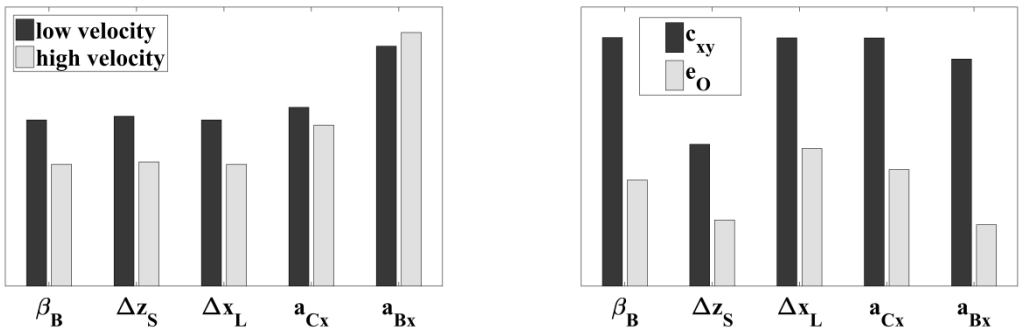

Figure 4. a) normalized m_O for two systems linearized at a low longitudinal velocity and a high longitudinal velocity, respectively; b) normalized c_{xy} and e_O for the first braking scenario in chapter 3.1.

4 CONCLUSION AND OUTLOOK

In the preceding sections a new observability measure is defined and applied to the longitudinal dynamics of a railway bogie. Some advantages as well as weaknesses of the newly developed index are presented. The results support a reasonable choice of the most characteristic and influential dynamic effects that might be measured and used as observer inputs.

Based on the presented and compared observability measures, the upcoming step to further enhance the envelope index is to extend it to the evaluation of an entire sensor configuration with multiple sensors. Another task to be tackled in the future is an upgrade of the index, so that it is able to incorporate sensor resolution and accuracy.

5 ACKNOWLEDGEMENTS

This work was supported by StMWi (StMWi Förderkennzeichen: MST-1308-0006// BAY 191/002), the Bavarian Ministry of Economic Affairs and Media, Energy and Technology, within the project DynORail.

REFERENCES

Alstom 2015 (online; accessed June 12 2017). Bogie catalogue. http://www.alstom.com/Global/Transport/Resources/Documents/brochure2014/Alstom%20Bogies%20Catalogue%202015%20-%20English.pdf?epslanguage=en-GB

Bendat, J.S. & Piersol, A.G. 1993. *Engineering applications of correlation and spectral analysis*. New York: John Wiley & Sons, Inc.

Benninger, N.F. & Rivoir, J. 1986. Ein neues konsistentes Maß zur Beurteilung der Steuerbarkeit in linearen, zeitinvarianten Systemen. *Automatisierungstechnik* 34: 473–479.

Bombardier 2007 (online; accessed June 12 2017). FLEXX Eco Bogies. http://www.bombardier.com/content/dam/Websites/bombardiercom/supporting-documents/BT/Bombardier-Transportation-Bogies-FLEXX-Eco.pdf

Bombardier 2008a (online; accessed June 12 2017). FLEXX Bogies. http://www.bombardier.com/content/dam/Websites/bombardiercom/supporting-documents/BT/Bombardier-Transportation-Bogies-FLEXX-High-Speed.pdf

Bombardier 2008b (online; accessed June 12 2017). FLEXX Link Bogies. http://www.bombardier.com/content/dam/Websites/bombardiercom/supporting-documents/BT/Bombardier-Transportation-Bogies-FLEXX-Link.pdf

Brembeck, J., Pfeiffer, A., Fleps-Dezasse, M., Otter, M., Wernersson, K. & Elmqvist, H. 2014. Nonlinear State Estimation with an Extended FMI 2.0 Co-Simulation Interface. *Proceedings of the 10th International Modelica Conference*: 53-62.

European Railway Research Institute - ERRI 1993. *B 176/3 Benchmark Problem: Results and Assessment*. ERRI B 176/DT 290.

Hac, A. & Liu, L. 1993. Sensor and actuator location in motion control of flexible structures. *Journal of Sound and Vibration* 167(2): 239-261.

Iwnicki, S. 1998. Manchester benchmarks for rail vehicle simulation. *Vehicle System Dynamics* 30: 295–313.

Kalker, J.J. 1982. A fast algorithm for the simplified theory of rolling contact. *Vehicle System Dynamics* 11: 1-13.

Lückel, J. & Müller, P.C. 1975. Analyse von Steuerbarkeits-, Beobachtbarkeits- und Störbarkeitsstrukturen linearer, zeitinvarianter Systeme. *Regelungstechnik* 23: 163–171.

Lystianingrum, V., Hredzak, B., Agelidis, V.G. & Djanali, V.S. 2014. Observability degree criteria evaluation for temperature observability in a battery string towards optimal thermal sensors placement. *IEEE 9th International Conference on Intelligent Sensors, Sensor Networks and Information Processing*: 1-6.

Polach, O. 1999. A fast wheel-rail forces calculation computer code. *Vehicle System Dynamics* 33: 728-739.

Siemens 2017 (online; accessed June 12 2017). First class bogies. https://www.mobility.siemens.com/mobility/global/SiteCollectionDocuments/en/rail-solutions/components-and-systems/bogies-catalog-en.pdf